JOURNAL OF CATALYSIS **161,** 524–529 (1996)
ARTICLE NO. 0214

Influence of the Amount of Titania on the Texture and Structure of Titania Supported on Silica

R. Castillo, B. Koch,* P. Ruiz, and B. Delmon

*Unité de Catalyse et Chimie des Matériaux Divisés, Université Catholique de Louvain, Place Croix du Sud 2/17, 1348 Louvain-la-Neuve, Belgium; and *Laboratoire Central, Solvay & Cie, Rue de Ransbeek 310, 1120 Brussels, Belgium*

Received November 21, 1994; revised March 15, 1996; accepted March 18, 1996

Samples obtained by grafting various amounts of titania over silica using titanium IV isopropoxide in isopropyl alcohol were studied using SBET, pore volume, XRD, ESCA, DRS, and zeta potential measurements. Very good dispersion of TiO_2 over silica approaching monolayer dispersion was observed for TiO_2 content lower than about 15 wt%. At higher TiO_2 content, TiO_2 crystallites were formed. A strong oxide–oxide interaction with the formation of the Ti–O–Si bond was observed. For a part of TiO_2, the intensity of this interaction increases with the calcination temperature, but for other parts, formed crystallites. © 1996 Academic Press, Inc.

1. INTRODUCTION

Titania-supported silica presents an increasing interest as a catalytic support (1–4). Reichmann and Bell (1) studied the factors that influence the phase structure of supported titania and concluded that the final structure obtained depends on stable intermediates formed during the impregnation of silica. Fernandez *et al.* (2) observed that highly dispersed TiO_2 phases supported on SiO_2 can be prepared by reacting titanium (IV) alkoxides, $Ti(OR)_4$, with the SiO_2 surface and calcination in air. Muñoz and Munuera (3) found that the incipient impregnation of SiO_2 with an *n*-hexane solution of titanium (IV) isopropoxide, $Ti(OPr^i)_4$, leads to TiO_2-coated material with an extremely high dispersion. Wauthoz *et al.* (4) showed that the impregnation of silica with titanium (IV) normal propoxide, $Ti(OC_3H_7)_4$, results in the formation of TiO_2 agglomerates and a poor titania dispersion.

In a previous work (5) we studied the deposition of titanium over silica using three methods: precipitation with $TiCl_4$ and ammonium hydroxide in aqueous solution, grafting with titanium (IV) isopropoxide in isopropyl alcohol, and grafting with a solution of $TiCl_4$ in *n*-hexane. We have shown that the method of deposition influences deeply the morphology and dispersion of the coated oxide. With the precipitation method, TiO_2 is deposited at the external parts of the silica particles. When $TiCl_4$ is used for grafting, the best internal TiO_2 dispersion together with formation of large crystallites at the external surface of silica are observed. The grafting with titanium (IV) isopropoxide in isopropyl alcohol provides the best external superficial dispersion of titania, allowing for the formation of small crystallites. In addition, a strong oxide–oxide interaction with formation of Ti–O–Si occurs.

In this work, we present further results concerning the influence of the amount of titania deposited on silica on the texture and structure of titania. We used the grafting method with titanium (IV) isopropoxide in isopropanol. Special attention has been given to the interaction between titanium oxide and silica.

Samples were characterized by the following physicochemical methods: BET surface area, pore volume, X-ray diffraction (XRD), electron spectroscopy for chemical analysis (ESCA), UV–Vis diffuse reflectance spectroscopy (DRS), and zeta potential measurements.

2. CATALYST PREPARATION

A silica support from Grace (BET surface area of 320 m^2/g) was used. The silica was first calcined in air at 600°C for 12 h before deposition of titania. The grafting method consisted of reacting the titanium alkoxide with the hydroxylated surface of silica. The support was added to a solution containing the necessary amount of titanium IV isopropoxide in isopropyl alcohol. After being stirred, the alcohol was removed by evaporation in a rotavapor at 70°C. The resulting solid was dried at 120°C for 12 h and calcined at 500°C for 20 h.

Samples containing between 2.0 and 20.0 wt% of TiO_2 over silica were prepared. All samples were prepared in a dry N_2 atmosphere. $Ti(OPr^i)_4$ and isopropanol (purity higher than, respectively, 98 and 99%, spectrophotometric grade) provided by Janssen Chimica were used. A part of the samples was recalcined at 815°C for 8 h.

For comparison purposes, a sample was prepared as a physical mixture ($TiO_2 + SiO_2$) containing 15 wt% of TiO_2 (anatase), commercial grade, BET surface area of 55.4 m^2/g.

0021-9517/96 $18.00

3. SAMPLE CHARACTERIZATION

3.1. Specific Surface Area BET and Pore Volume

Measurements were carried out in a Micromeritics Asap 2000 equipment at −196°C using nitrogen as adsorption gas.

3.2. Electron Spectroscopy for Chemical Analysis

The X-ray photoelectron spectra were performed at room temperature with a photoelectron spectrometer SSI X-probe(SSX-100/206) of Fisons, interfaced to a Hewlett–Packard 9000/310 computer. A monochromated Al anode (energy of the Al$K\alpha$ line 1486.6 eV) source, operating at 10 keV and 12 mA, was used for X-ray production. Samples were compressed in small cups, supported horizontally on a holding carousel. The binding energy scale of the spectrometer was calibrated with the Au4$f_{7/2}$ line (binding energy 83.98 eV). The spot size was around 1.4 mm^2 and the pass energy was set at 50 eV: under these conditions the resolution determined by the full width at half-maximum of the Au4$f_{7/2}$ peak of a standard gold sample was around 1.1 eV. The positive charge, developed on our nonconductive samples due to the photoejection process, was compensated by a charge neutralizer. A low-energy flood gun whose energy was adjusted at 6 eV (50 μA) with a Ni grid placed 3 mm above the samples was used to control charging on the sample surface. The stability of charge compensation as a function of time was controlled by recording the C1s line at the beginning and the end of the analysis of each sample: the displacement of peak position is always less than 0.1 eV (6). The pressure inside the analysis chamber was about 3×10^{-7} Pascal. The Cls, Ols, Si2p, Ti2p, and Cls lines were measured and their binding energies were referenced to the Cls peak (C–C, C–H) set at 284.8 eV. Atomic concentration ratios, $(\mathrm{Ti/Si})_{\mathrm{ESCA}}$, were calculated by correcting the measured intensity ratios with the theoretical sensitivity factors based on Scoffield cross sections (7). Decomposition of peaks was done with the best fitting routine of the SSI instruments.

The theorical XPS intensity ratio of Ti2p/Si2p was calculated by the sheet model for dispersion of the catalyst particles proposed by Kerkhof and Moulijn (8) corresponding to the equation

$$\frac{I_{\mathrm{Ti}}}{I_{\mathrm{Si}}} = \frac{n_{\mathrm{Ti}}}{n_{\mathrm{Si}}} \times \frac{D_{\mathrm{Ti}}}{D_{\mathrm{Si}}} \times \frac{\sigma_{\mathrm{Ti}}}{\sigma_{\mathrm{Si}}} \times \frac{1}{(\rho_{\mathrm{Si}} S_{\mathrm{Si}} \lambda_{\mathrm{Si}})} \times \frac{(1 + \exp(-2/\rho_{\mathrm{Si}}\lambda_{\mathrm{Ti}}S_{\mathrm{Si}}))}{(1 - \exp(-2/\rho_{\mathrm{Si}}\lambda_{\mathrm{Ti}}S_{\mathrm{Si}}))}.$$

In this equation, $n_{\mathrm{Ti}}/n_{\mathrm{Si}}$ is the atomic ratio of Ti and Si. D_{Ti} and D_{Si} are the spectrometer detection efficiencies for the corresponding photoelectrons. D is inversely proportional to the electron kinetic energy. σ_{Si} and σ_{Si} are the respective photoelectron cross sections. λ_{Ti} and λ_{Si} are the respective photoelectron escape depths. ρ_{Ti} and ρ_{Si} are the densities of TiO_2 and SiO_2, respectively. S_{Si} is the specific surface area of SiO_2.

The equation was used using the photoionization cross sections determined by Scofield (7) and the ratio of mean free path for electrons determined by Penn (9).

For monolayer catalysts a linear relation between the theoretical relative XPS intensity (given by the model) and bulk atomic ratio can be expected for a series of catalysts with increasing titanium content. The fact that the experimental relative XPS intensity is lower than those predicted by the model may be explained in terms of crystallite growth (8, 10).

3.3. Zeta Potential

Zeta potential measurements were carried out in a PEN KEM Zeta Meter 500 using 25 mg of sample ultrasonically dispersed in 200 ml of an aqueous solution containing 10^{-3} M KCl. The pH was adjusted with 10^{-3} M solutions of KOH or HCl. The zeta potential values were obtained from electrophoretic migration rates using Smoluchowski's equation (11). The isoelectric point (IEP) was taken as the pH at which the overall surface charge of the solid was zero (zero rate of migration). The apparent surface coverage (ASC) of TiO_2 over the silica was calculated by using the equation

$$\%\mathrm{ASC} = M_{\mathrm{Ti}}(\mathrm{IEP_{Si}} - \mathrm{IEP_{Ti/Si}})/ ((M_{\mathrm{Si}}(\mathrm{IEP_{Ti/Si}} - \mathrm{IEP_{Ti}}) - M_{\mathrm{Ti}}(\mathrm{IEP_{Ti/Si}} - \mathrm{IEP_{Si}})),$$

where M_{Ti} and M_{Si} are the molecular weights of titania and silica, respectively, and the subscript Ti/Si is the analyzed sample. The surface area developed by the supported TiO_2 was calculated as the product of ASC value and BET value of the sample (5).

3.4. UV–Vis Diffuse Reflectance Spectroscopy

UV–Vis diffuse reflectance spectra were obtained with the reflectance attachment of a CARY 1756 spectrometer connected to a Hewlett–Packard computer. The spectra were recorded between 210 and 700 nm using $BaSO_4$ as reference. Absorption spectra are presented with units of absorption as ordinates and units of wavelength as abscissas. The position of the absorption maxima has been used to characterize the absorption edge.

3.5. X-Ray Diffraction

X-Ray diffraction spectra were taken on a Philips PW 1050 diffractometer connected to a computer. The spectra were taken using the Cu$K\alpha$ line.

4. RESULTS

4.1. BET Analyses

Figure 1 shows the specific BET surface area and pore volume for different titania loadings on silica. Both

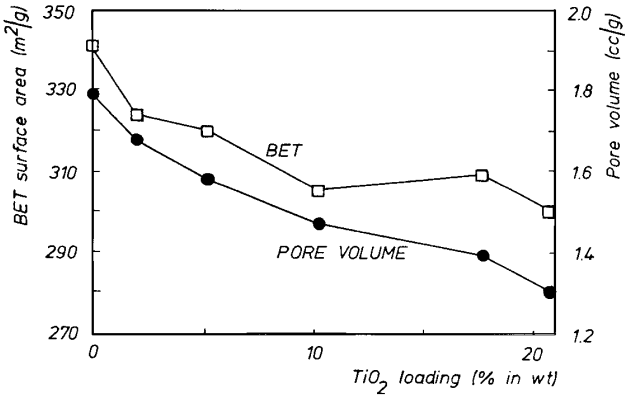

FIG. 1. BET surface area and pore volume as a function of the percentage of TiO_2 loading by weight.

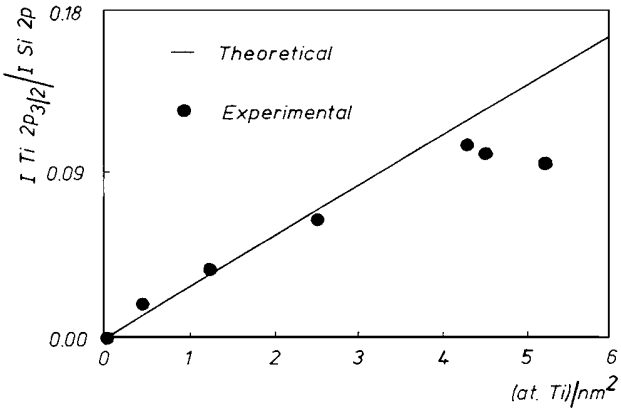

FIG. 2. Calculated and measured XPS intensities. *Y*-axis is the XPS Ti/Si atomic ratios. *X*-axis is the number of Ti atoms by the surface area of silica.

diminished when the TiO_2 content increases. The diminution of the BET area due of the deposition of titania is less drastic when the TiO_2 loading varies between 10 and 22 wt%.

4.2. ESCA

ESCA results are presented in Table 1. For various titanium dioxide contents, binding energies are in agreement with the binding energy of Ti^{4+} (458–459 eV) reported by Wauthoz *et al.* (4), Raupp and Dumesic (12), Mukhopadhyay and Garofalini (13), and Wei *et al.* (14). On the other hand, in samples containing titanium, all binding energies of Ti2*p* are from 0.8 to 1.9 eV higher than those observed in pure anatase. In addition, the binding energy of titanium increases when the loading in TiO_2 decreases. When the samples containing 5.2 and 17.8 wt% to TiO_2 were subjected to calcination at 815°C for 8 h, an increase in the shift of Ti2*p* binding energy of 0.5 and 0.6 eV, respectively, was observed.

The theoretical and measured ESCA Ti2*p*/Si2*p* intensities are presented in Fig. 2. The experimental points corresponding to the samples containing less than 17.8% of TiO_2 are on the straight line. They are under the straight line for the higher titania.

Figures 3 and 4 show the O1*s* line spectra for the mechanical mixture (15 wt% TiO_2) and for the sample 17.8 wt% TiO_2 calcined at 815°C, respectively. Figure 3 shows that the difference between the binding energies of the two components of the O1*s* line spectra is 3.6 eV. The larger peak coincides with the position of the pure SiO_2 peak (532.97 eV), and the smaller peak (529.36 eV) with the O1*s* line for the Ti–O bond in TiO_2. In Fig. 4, the two components can also be observed, but the difference between the two peaks is only 2.4 eV. The larger peak at 532.90 eV corresponds to the O1*s* line of pure SiO_2 (Si–O–Si bond), but the smaller peak, at 530.53 eV, does not correspond to the expected value for TiO_2. This observed binding energy could be attributed to the Ti–O–Si bond, according to Mukhopadhyay and Garofalini (13) and Mohai *et al.* (15).

TABLE 1

XPS Analysis of Titania on Silica

Sample	%TiO_2	g Ti/g Si	at Ti/nm^2	I(Ti2p)/I(Si2p)	BE (eV) Ti2$p_{3/2}$
	20.9	0.339	5.25	0.0916	458.9
	17.8	0.278	4.34	0.1048	458.8
Calcined at 815°C[a]	17.8	0.278	4.80	0.0836	459.3
	10.3	0.147	2.55	0.0641	459.3
	5.2	0.072	1.26	0.0370	459.3
Calcined at 815°C[a]	5.2	0.072	1.41	0.0356	459.9
	2.0	0.026	0.46	0.0180	459.3
TiO_2	100	—	—	—	458.0

Note. %TiO_2, percentage of TiO_2 loaded on the samples; g Ti/g Si, grams of titania by gram of silice; at Ti/nm^2, atoms of titania by surface area (in nm^2) of silica; I(Ti2p)/I(Si2p), XPS atomic ratio; and BE, binding energies of Ti2$p_{3/2}$ electrons.

[a] Samples calcined at 815°C for 8 h.

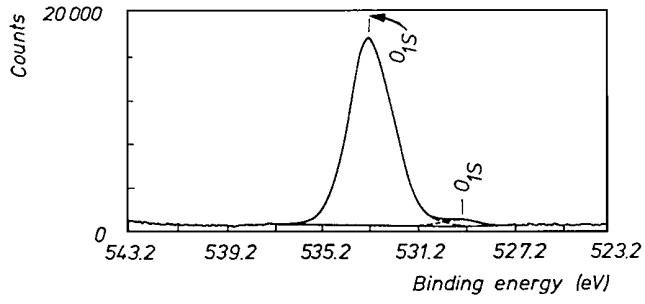

FIG. 3. O1*s* photoelectron peak from $TiO_2 + SiO_2$ mechanical mixture with 15 wt% TiO_2.

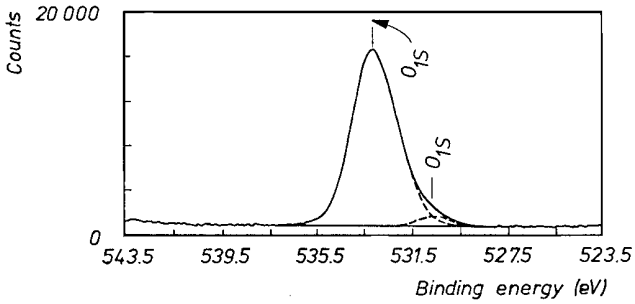

FIG. 4. O1*s* photoelectron peak from sample prepared by grafting containing 17.8 wt% of TiO_2 calcined at 815°C.

4.3. Zeta Potential

Figure 5 shows the variation of the ASC, as measured using zeta potential data, with the amount of TiO_2 deposited over silica. For a TiO_2 content of 20.9 wt%, about 85% of the surface of the sample is covered by titanium dioxide. For higher compositions the curve becomes assymptotic at about this value of ASC (85%).

4.4. UV–Vis Diffuse Reflectance

Figure 6 shows the absorption edge of the Ti–O charge transfer band for sample loadings of 5.2 and 17.8% and the mechanical mixture containing 15 wt% of TiO_2. In the mechanical mixture the absorption edge is observed at 320 nm. The sample with the 5.2 wt% loading shows an absorption edge near 290 nm; the sample with the 17.8 wt% loading shows both absorption edges (290 and 320 nm).

4.5. X-Ray Diffraction

Anatase crystallites are only detected in X-ray diffraction for a TiO_2 content of 17.8 wt% or higher. No peaks are detected at lower TiO_2 contents.

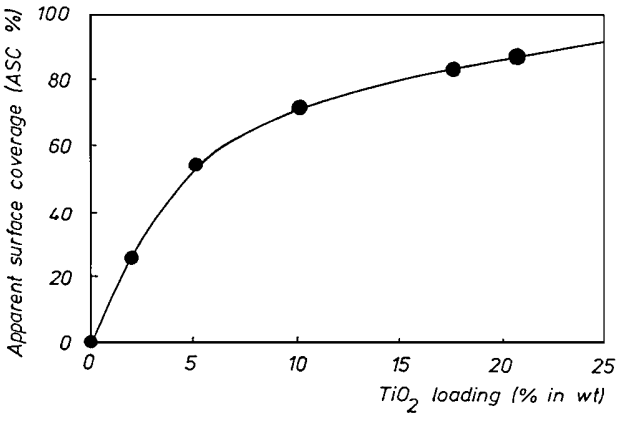

FIG. 5. Variation of the apparent surface coverage (ASC, in%) with the amount of TiO_2 loading over silica (wt%).

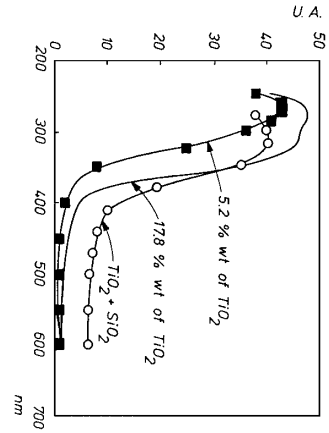

FIG. 6. UV–Vis diffuse reflectance. Absorption edge of Ti–O charge transfer band for samples loading 5.2 and 17.8 wt% of TiO_2 and the mechanical mixture containing 15 wt% of TiO_2. *Y*-axis is in arbitrary units. *X*-axis is absorption edge in nanometers.

5. DISCUSSION

5.1. Texture and Dispersion of Titania over Silica

The present results confirm the good dispersion of titania on the support using the alkoxide grafting method demonstrated by Castillo *et al.* (5).

The grafting using titanium (IV) isopropoxide provides a good dispersion of TiO_2 over silica for contents lower than about 15 wt%. These results are in accordance with other results presented by Muñoz and Munera (3) where the theoretical amount of titanium necessary to form a TiO_2 monolayer was calculated considering the density of the (010) plane of anatase (5.5 Ti^{4+} per nm^2). Taking this value into account, the amount of TiO_2 necessary to cover the surface of the silica used in this work with one monolayer is about 19.0 wt%.

This result is in agreement with the ESCA and the zeta potential analysis. ESCA results presented in Fig. 2 show that the experimental points containing less than 17.8 wt% are on the theoretical straight line, corresponding to a monolayer. For this titania content a good superficial dispersion of TiO_2 over the support is achieved with no indication that crystallites are present. This confirms the results obtained with the zeta potential analysis. The ASC values indicate that for samples containing 17.8 and 20.9 wt% of TiO_2 about 82 and 85 wt% of the surface is covered by titania, respectively.

The fact that a good dispersion is obtained is also confirmed by the XRD of samples containing less than 17.8 wt%. No line is involved.

However, a loss in surface area and in pore volume compared with pure silica is observed as a consequence of the deposition of titanium oxide. This must be attributed to the plugging of pores. We thus conclude that the majority of

titanium oxides form a monolayer on the surface of silica, but that a small proportion of titanium plugs the pores.

At higher TiO_2 amounts, experimental points are under the straight line in Fig. 2. This must be explained by the formation of TiO_2 crystallites, as shown by XRD observation, in confirmation of the observation of Kerkhof and Moulijn (8). The formation of TiO_2 cristallites can also be observed by calcining samples with a low titanium content (XRD).

5.2. Interaction between Titania and Silica: Formation of the Ti–O–Si Bond

A significant result is the increase by about 0.8 to 1.9 eV of the binding energy for the titanium-coated samples when compared with pure TiO_2 (anatase) (Table 1). Actually, there is a small but significant decrease in the binding energy of Ti2$p_{3/2}$ electrons when the TiO_2 increases. This is easily explained. At lower contents, practically all titanium is in interaction with SiO_2. The high binding energy reflects the fourfold coordination of Ti in the strongly interacting Ti–O–Si. At higher loadings, increasing contributions of the sixfold contribution of Ti^{4+} to oxygen in pure TiO_2 (rutile or anatase) led to a decrease of the binding energy.

This conclusion is supported by results obtained by DRS analyses (Fig. 6). The sample containing 5.2 wt% of TiO_2 has an absorption edge at 290 nm (titanium in tetrahedral coordination). The sample containing 17.8 wt% of titanium shows both absorption edges (290 and 320 nm, respectively). The sample formed by the mechanical mixture of 15 wt% TiO_2 (anatase) and SiO_2 shows the absorption edge of the Ti–O charge transfer band at 320 nm (titanium in octahedral coordination Mukhopadhyay and Garofalini (13)). This interpretation is confirmed by the conclusions of Fernandez *et al*. (2) and Forger and Anderson (16) when they discuss changes in the environment of Ti^{4+}.

The association of titania and silica via the formation of the Ti–O–Si bond strongly depends on the amount of TiO_2 present on the support. The work of Greegor *et al*. (17) and Sandstrom *et al*. (18) over titania–silica glasses showed that, for samples containing titanium in amounts as high as 9 wt%, Ti^{4+} occupied a tetrahedral coordinated site similar to that of Si in SiO_2, while maintaining a small fraction (less than 5%) in octahedral coordination. Above 9 wt% TiO_2, the octahedral/tetrahedral ratio increased appreciably, and at 15 wt% an identifiable rutile- or anatase-like structure was formed as a second phase (17, 18).

These changes in the coordination (or in the nature of ligands) of titanium induce changes on the O1*s* photoelectron peak associated to Ti (Figs. 3 and 4). Since Ti is more electropositive in nature than Si, the core electron-binding energy of the oxygen atom is reduced when a Si–O–Si bond is replaced by a Ti–O–Si, bond. The Ti–O bond may then be more ionic in character, thus making the oxygen atom slightly more negative, explaining the shift in the O1*s* photoelectron peak.

In conclusion, the shifts in the binding energies observed in the present work can be attributed principally to the different coordination number (or nature of ligands) of titanium by formation of Ti–O–Si bonds.

However, the shift of binding energy of the Ti2*p* photoelectrons may be explained also in another way. Anpo *et al*. (19), who studied the TiO_2/Al_2O_3 system, explained the shifts in the binding energies of Ti2*p* electrons (about 1 eV) by a change of the relaxation energy of TiO_2 species due to their high dispersion on the Al_2O_3 carrier matrix.

Our suggestion is that, as has been shown previously by Mukhopadhyay and Garofalini (13), Mohai *et al*. (15), Greegor *et al*. (17), and Sandstrom *et al*. (18), the shift in the binding energy of the Ti2*p* photoelectrons is produced when titanium is associated to silica in the Ti–O–Si bond.

Results obtained with calcined samples seem to confirm our proposal rather than the interpretation of Anpo *et al*. (19). The samples of 5.2 and 17.8 wt% of TiO_2, when subjected to a calcination at 815°C for 8 h, show an increase in the binding energy of Ti2$p_{3/2}$ photoelectrons of 1.9 and 1.3 eV, respectively, when compared with the titanium in pure anatase. Simultaneously, a crystallization of TiO_2 on the surface occurs during calcination. The signal corresponding to Ti in strong interaction with Si increases in comparison with that of TiO_2 crystallites. This enhances the signal of the TiO_2 monolayer. The observed shift is to be attributed to the contribution of the Ti–O–Si bonds. As a whole, the change in the chemical environment of Ti^{4+} is favored by the increase in calcination temperature.

6. CONCLUSIONS

The grafting of a silica of a 320 m^2/g surface area with titanium IV isopropoxide in isopropanol allows for a very good, near-monolayer TiO_2 dispersion at contents lower than 17.8 wt%.

There is a strong oxide–oxide interaction between Ti and Si due to the formation of Ti–O–Si bonds. The degree of this interaction decreases with the TiO_2 content and increases with the calcination temperature.

The Ti^{4+} species can be tetrahedrally and/or octahedrally coordinated. The octahedral coordination corresponds to TiO_2 crystallites. It is favored only at a high concentration of titanium.

REFERENCES

1. Reichmann, M. G., and Bell, A. T., *Appl. Catal.* **32**, 315 (1987).
2. Fernandez, A., Leyrer, J., Gonzalez, A., Muñera, G., and Knözinger, H., *J. Catal.* **112**, 489 (1988).
3. Muñoz, A., and Munera, G., "Studies in Surface Science and Catalysis. No. 63. Preparation of Catalysts V" (G. Poncelet, P. A. Jacobs, P. Grange, and B. Delmon, Eds.), p. 627. Elsevier, Amsterdam, 1991.
4. Wauthoz, P., Ruwet, M., Machej, T., and Grange, P., *Appl. Catal.* **69**, 149 (1991).
5. Castillo, R., Koch, B., Ruiz, P., and Delmon, B., *J. Mater. Chem.* **4**(6), 903 (1994).

6. Bryson, C. E., III, *Surf. Sci.* **189/190**, 59 (1987).
7. Scofield, J. H., *J. Electron Spectrosc. Relat. Phenom.* **8**, 129 (1976).
8. Kerkhof, F. B., and Moulijn, J. A., *J. Phys. Chem.* **83**, 1612 (1979).
9. Penn, D. R., *J. Electron Spectrosc. Relat. Phenom.* **9**, 29 (1976).
10. Siuda, R., "Surface Science," Vol. 177, p. L1011. North-Holland, Amsterdam, 1976.
11. Smoluchowski, M., *in* "Handbuch der Elektrizität und der Magnetism" (B. Gractz, Ed.), Vol. 2, p. 366. Leipzing, 1914.
12. Raupp, G. B., and Dumesic, J. A., *J. Phys. Chem.* **89**, 5240 (1985).
13. Mukhopadhyay, S., and Garofalini, S., *J. Non-Cryst. Solids* **126**, 202 (1990).
14. Wei, Z., Xin, Q., Guo, X., Sham, E., Grange, P., and Delmon, B., *Appl. Catal.* **63**, 305 (1990).
15. Mohai, M., Bertóti, I., and Révész, M., *Surf. Interface Anal.* **15**, 364 (1990).
16. Forger, K., and Anderson, J. R., *Appl. Catal.* **23**, 139 (1986).
17. Greegor, R., Lytle, F., Sandstrom, D., Wong, J., and Shultz, P., *J. Non-Cryst. Solids* **55**, 27 (1983).
18. Sandstorm, D., Lytle, F., Wei, P., Greegor, B., Wong, J., and Shultz, P., *J. Non-Cryst. Solids* **41**, 201 (1980).
19. Anpo, M., Kawamura, T., Kodoma, S., Maruya, K., and Onishi, T., *J. Phys. Chem.* **92**, 438 (1988).